Annales Geophysicae (2003) 21: 2043–2057

Annales Geophysicae

Ion cyclotron waves in the Earth's magnetotail during CASSINI's Earth swing-by

A. T. Bogdanov[1], K.-H. Glassmeier[1], G. Musmann[1], M. K. Dougherty[2], S. Kellock[2], P. Slootweg[2], and B. Tsurutani[3]

[1]Institute for Geophysics and Meteorology, Technical University of Braunschweig, Mendelssohnstrasse 3, 38106, Braunschweig, Germany
[2]Imperial College of Science and Technology, London, UK
[3]Jet Propulsion Laboratory, California Institute of Technology, Pasadena, USA

Received: 12 September 2002 – Revised: 3 March 2003 – Accepted: 8 April 2003

Abstract. The properties of low frequency magnetotail waves observed during CASSINI's Earth swing-by are examined. A maximum in the distribution of the waves about half the proton cyclotron frequency and a peak at linear polarisation are found and their implications are analysed in detail. Data on the fluid plasma velocity for the observation interval are not available and thus no unique conclusions about Doppler shift influence on the properties of the waves can be made. This determines the need to analyse different hypotheses in order to understand the origin of the waves. The plausibility of competing interpretations, such as off-resonance proton cyclotron waves and bi-ion cyclotron waves at the gyrofrequency of a heavy ion component of the magnetotail plasma in the form of He^{++} ions of solar wind origin is questioned.

Key words. Space plasma physics (waves and instabilities) – Magnetospheric physics (plasma waves and instabilities; magnetotail)

1 Motivation

In their work on LF electromagnetic ion cyclotron waves (EMIC) Tsurutani et al. (2002) point out the observation of two new modes of magnetotail low frequency waves, an almost purely compressional mode and a transverse one, both in the proton cyclotron frequency range.

We take their statement as a starting point for this study, aiming at a more detailed picture of the plasma properties of the magnetotail regions traversed by CASSINI via a statistical analysis of the observed waves. Another point, which makes the present investigation interesting, is that, in spite of the several decades of magnetospheric studies, observations from the intermediate ranges of the magnetotail, between 20 R_E and 60 R_E, especially in this frequency interval are sparse. Most of the existing work concentrates on the near-Earth magnetotail: Angelopoulos et al. (1989), Chaston et al. (1994, 1999) or on the outer reaches beyond 150 R_E: Tsurutani et al. (1985), Kawano et al. (1994).

In August 1999 the combined Saturn-Titan Mission satellite CASSINI-HUYGENS flew by the Earth in a swing-by acceleration manoeuvre on its way to Saturn. This was an excellent opportunity for testing of the instrumentation and for a new perspective on the Earth's magnetosphere in a very quick snapshot-like flyby, to a high degree coaxial with the Earth's magnetotail at a velocity of ∼16.1 km/s. Almost all of the important magnetospheric structures pertaining to the equatorial inner magnetosphere and to the near-to-the-plasma sheet space of the magnetotail were inspected. The overall picture of these observations from a magnetic field point of view has already been drawn in publications by Southwood et al. (2001), and Tsurutani et al. (2002). An exhaustive correlative study of the magnetospheric plasma system as a whole during the flyby period is presented in Khan et al. (2001).

In our work we shall turn to a well-defined – both in its space and frequency range – region of investigation. We shall look into the magnetotail as seen by CASSINI from the moment in which the spacecraft is leaving the dipolar magnetic field of the inner magnetosphere at about 04:15 UT, up to its final departure from the magnetotail at about 10:47 UT on 18 August 1999, Fig. 1. Our primary interest lies with waves of the ion cyclotron type. The latter were already investigated for the region of the subsolar magnetosheath and the dayside boundary region by Southwood et al. (2001) and Tsurutani et al. (2001). The second of these contributions has, in fact, covered the flyby trajectory as far as the moment of leaving the dipolar region of the magnetosphere.

Magnetic field fluctuations in the frequency range about the cyclotron frequency of the dominant ion species of the ambient plasma are not a new subject in magnetotail physics. The near-Earth and distant magnetotail and its plasma sheet and plasma sheet boundary layer in particular, have been studied experimentally using ISEE data by Tsurutani et al. (1985), Cattell et al. (1986), Elphic and Gary (1990), and Chaston et al. (1994). AMPTE/IRM data underlie statistical

Correspondence to: A. T. Bogdanov (a.bogdanov@tu-bs.de)

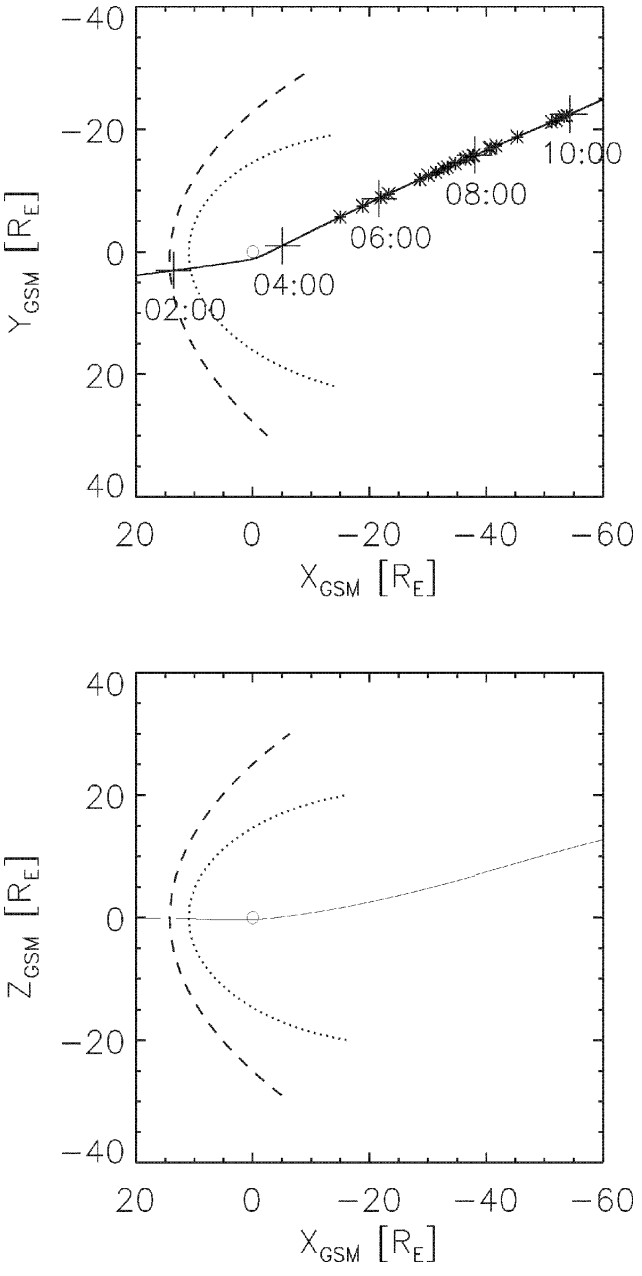

Fig. 1a. Overview of the timing of the wave events and CASSINI's trajectory during the Earth swing-by manoeuvre in GSM reference frame. Cross sections in the $x - y$ and $x - z$ planes are shown on the background of a model bowshock and magnetopause.

studies by Bauer et al. (1995) and Neagu et al. (2001). The properties of the waves to be found there were discussed from a dispersion theory point of view in papers by Angelopoulos et al. (1989), Gary (1991), and Chaston et al. (1999). Simulation work on ion instabilities possible under magnetotail conditions has been reported by Gary and Winske (1990), Gary et al. (1993, 1994), Gary and Lee (1994). Because of the multi-ion character of the plasmas in the inner magnetosphere and the near-Earth magnetotail, the dispersion in the low frequency range of multi-ion plasmas has also received considerable attention in works by Smith and Brice (1964), Young et al. (1981), Gomberoff and Neira (1983), Kozyra et al. (1984), Chaston et al. (1997). Ion cyclotron heating of heavy ions by ion waves has been discussed by Chaston et al. (2000). We shall see that these contributions constitute the basis for understanding our observations.

2 Magnetic field data

The Flux Gate Magnetometer (FGM), data of which are used in this study, has been described by Kellock et al. (1996). We use here data averaged over 1 s – sufficient to study waves at magnetotail proton gyrofrequencies in the range of tenths of Hz, with the proton cyclotron period at 5–20 nT being about 12.0–3.5 s.

We are interested in the time interval 18 August 1999, 04:15–10:45 UT. Figure 1a displays in $x - y$ and $x - z$ GSM-projection the spacecraft trajectory, as well as those locations where the LF waves have been observed. Model bowshock and magnetopause configurations are also shown. The observation conditions and the temporal behaviour of the magnetic field become clear from Fig. 1b, on which the magnitude and the magnetic field components in GSM representation, sampled at 1 s rate, are plotted. According to Khan et al. (2001) two substorms occurred between 03:45–06:45 UT and 06:45–09:45 UT. The spacecraft exits the magnetosphere at 10:47 UT after crossing a region of strong disturbances coupled to the magnetopause current layer. Another very disturbed region is present in the data between 09:05 UT and 09:14 UT, when a temporary dive into the magnetosheath occurs. In the remaining time the spacecraft is well within the northern magnetotail.

Due to the substorm activity, it is difficult to locate the s/c with respect to the different magnetotail regions based on magnetic field data only. Here we use the identifications given by Khan et al. (2001) based on plasma observations: about 2/3 of the time spent in the magnetotail CASSINI was within the plasma sheet (PS), leaving it for a few minutes after 07:33 UT and finally at 08:10 UT, to enter the northern lobe. All wave events studied belong to the substorm periods with the exception of a few observed after the end of the second substorm at about 09:45 UT (Fig. 1).

3 Data analysis

The observed wave trains are characterised by short lifetimes. Even in the case when the oscillations persist without changing frequency, phase slips destroy the coherence and render a coherent wave packet duration of more than 3–4 cycles impossible. Therefore, we abstain further from using the classical Fourier decomposition of the signals. We shall instead rely on results from principal component analysis in the time domain to deduce the fundamental wave characteristics. Concerning the reason for the relatively short periods in which coherent wave activity can be observed, with single point measurements, we can only speculate whether the

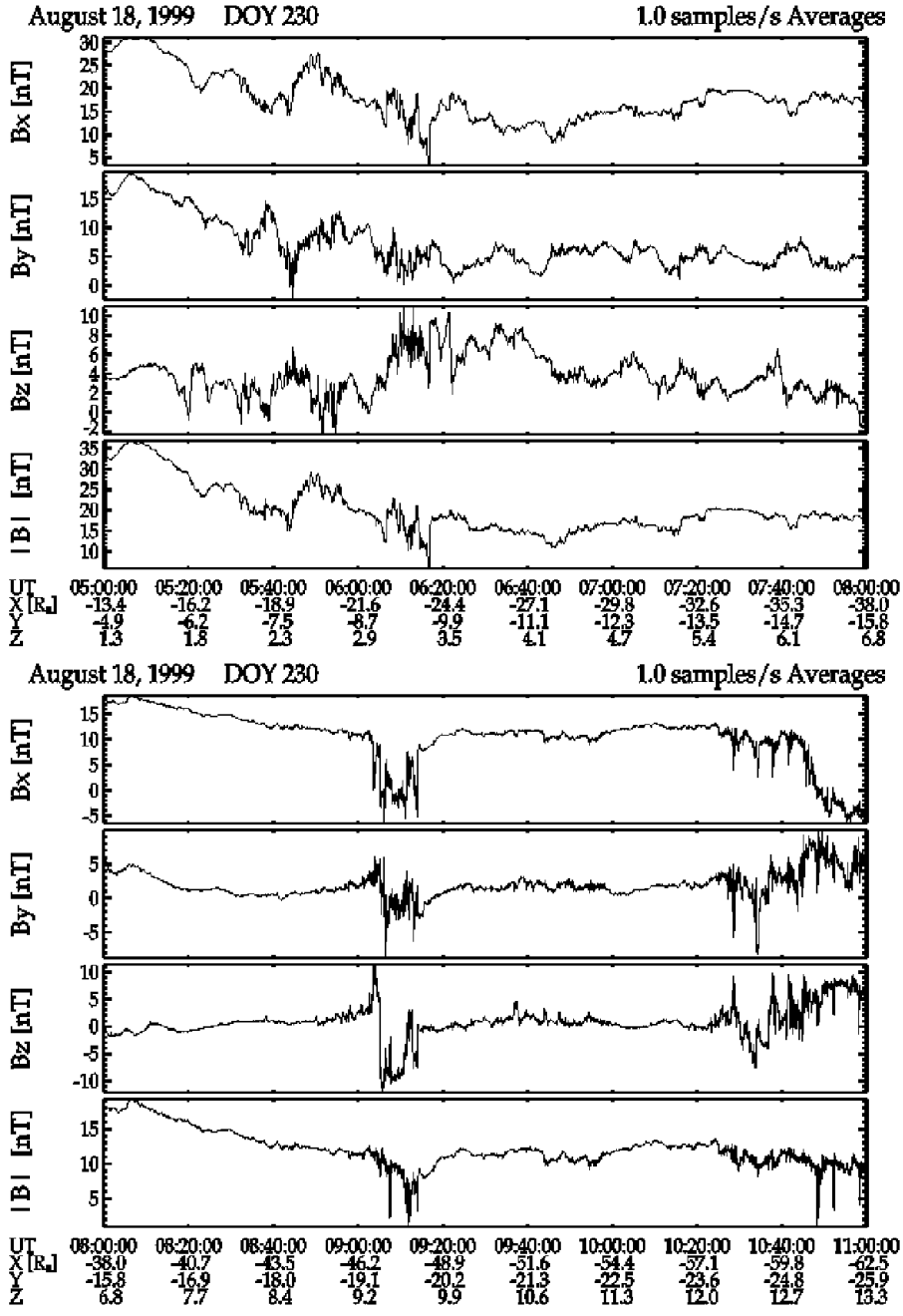

Fig. 1b. The overall temporal behaviour of the magnetic field components and the field magnitude in GSM reference frame. The period of the first plot coincides roughly with the plasma sheet passage and the second one belongs to the flyby through the northern magnetotail lobe.

lifetimes of the observed wave structures reflect their spatial extent or the brevity is a consequence of the waves being carried away by plasma streaming. We can only exclude the spacecraft's own motion as the cause, due to its own negligible velocity compared to the speed of plasma flows in the magnetotail region.

We shall call the data point sequences, which are analysed separately, "wave events" or simply "events". To avoid misunderstandings, it should be explicitly stated here that this is a narrower definition, compared to the usage of the term by other authors. Anderson et al. (1996) and Denton et al. (1996), in papers on the effects of wave superposition on the observed polarisation, use the word in the sense of a prolonged period of observation during which a continuous sequence of superpositions of linear wave states of similar polarisation characteristics is observed and analysed as a series in time of distinct points in the wave parameter space. Each of these points reflects a short period of 2–3 wave oscillations, called a "wave step". The statistical properties of each of their events are derived by analysing the set of wave

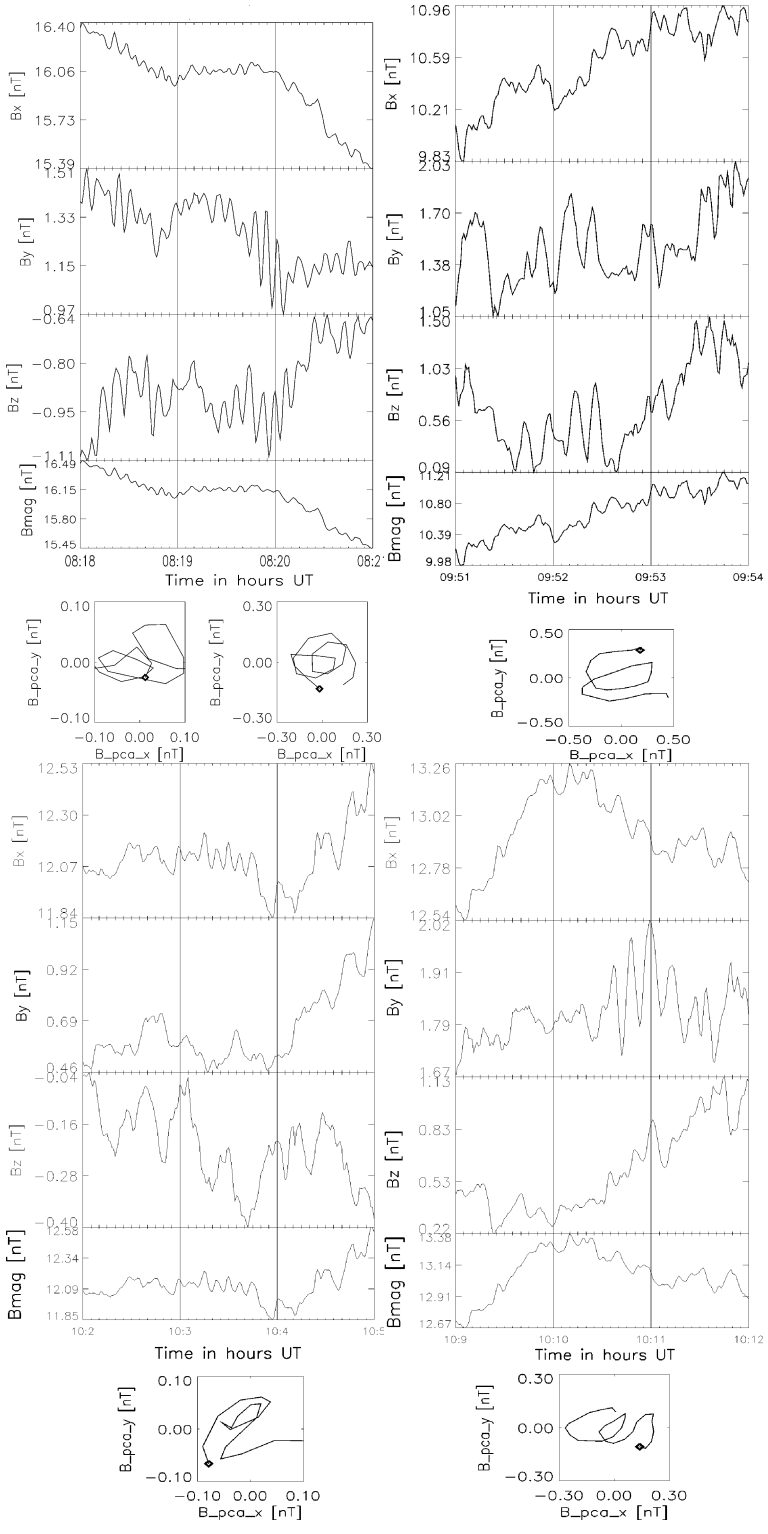

Fig. 2. Examples of the wave bursts seen by CASSINI's magnetometer within its magnetotail journey; the time series are in GSM coordinates while the respective hodograms represent the magnetic field vector projected in the plane perpendicular to the minimum variance direction; **(a)** two events, 08:19:20–08:19:43 UT (the left-hand side hodogram) and 08:19:45–08:20:07 UT (the right-hand side hodogram); **(b)** wave event in the interval 09:52:07–09:52:33 UT; **(c)** wave event: 10:03:15–10:03:35 UT; **(d)** 10:10:37–10:11:07 UT.

steps belonging to it. Differently, we use the term to denote an observation of a short-lived wave sequence, similar in its duration to the "wave step". For lack of long and time-continuous series of such events, although they are obviously not the manifestation of "pure" wave states, we do not have a better choice but to assume they can be approximated by single (pure) monochromatic wave modes in the sense of these authors. We classify the waves according to their main parameters, such as wave frequency, propagation angle, and ellipticity.

The frequency is derived directly from the duration and the number of periods over which a certain wave event is observed. The propagation angle θ_{kB} is defined as the angle between the minimum variance direction (assumed to be the wave propagation direction) and the averaged magnetic field vector. All values larger than 90° are substituted by their values complementary to 180°.

The ellipticity is defined as the ratio of the intermediate to maximum eigenvalues of the principal component analysis multiplied by ± 1 for the right-hand/left-hand rotating field vector in the plane perpendicular to the minimum variance direction, with the normal to the plane chosen to have an angle to the average magnetic field of less than 90°.

A careful visual inspection of the analysis interval provides one with more than 40 wave packet sequences in the proton cyclotron frequency range. As a further criterion for including a certain wave event in our analysis we use minimum variance analysis and study only those events for which the ratio of the intermediate to the minimum eigenvalues is larger than 3. This ratio indicates the degree to which the magnetic field oscillations can be approximated by a single plane wave. The general experience with minimum variance analysis recommends a value as high as 10 (Sonnerup and Scheible, 1998). We compromise on this requirement since only about 20% of the events identified fulfil this very strict criterion. At a level of 3, the number of events included in our statistics is reduced to 24.

A note on the observation conditions is also necessary. For the measurements presented here Doppler shifts caused by the motion of the satellite are of practically no importance, as the Alfvén velocity in the ambient plasma is on the order of several hundred km/s while the spacecraft moves at some 16.1 km/s in the GSE reference system. More complicated is the question of possible Doppler shifts caused by the convective motion of the magnetotail plasma itself. Observations of the convection velocity are not available for the present study. However, convective velocities ($V_{\rm conv}$) observed earlier in the deep magnetotail have values which lie in the range of 0.1–1.0 times the local Alfvén velocity (Tsurutani et al., 1985). Thus, from the Doppler shift formula $f_{sc} = f_{\rm plasma}(1 + / - V_{\rm conv}/V_{\rm phase}\cos\theta_{kV}), \theta_{kV}$ – the angle between the wave vector $\boldsymbol{k}$ and the fluid velocity vector $\boldsymbol{V_{\rm conv}}$, and with phase velocities of the waves $V_{\rm phase} \sim V_{\rm Alfvén}$, it is obvious that the observed wave frequencies, f_{sc}, in the spacecraft reference frame, can substantially deviate from $f_{\rm plasma}$ – the frequency in the plasma. Since no observations of the actual convection velocity are available, this caveat of our investigation needs to be remembered. We shall comment on it at the end of the section on data analysis.

3.1 Sample wave events

To illustrate the waves under discussion we take a closer look at some examples. The observations are presented in Fig. 2 as time series of 3-min duration each, in GSM reference frame as well as hodograms of the field components in the $x - y$ plane perpendicular to the direction of minimum variance and for the short time intervals of the events only. A diamond, for the sake of determining the sense of rotation, marks the initial data point on each hodogram. The minimum variance coordinates have been chosen so that the z-direction of the right-hand oriented reference system is along the direction of minimum variance and makes an angle with B_o less than 90°.

In Fig. 2a we have four distinguishable wave trains (as already explained, we further call such sequences "events"). Two of them we leave for the statistics (08:18:18–08:18:43 UT and 08:20:32–08:20:51 UT) and the two between them are studied in detail. The first of them can be identified between 08:19:20 and 08:19:43 UT. The next one follows immediately in the interval 08:19:45–08:20:07 UT. In fact, were it not for the phase slip in-between, most prominent in the B_y-component of the magnetic field in GSM reference system, we could have regarded both of them as a single event. Since their compressibility ratio is also different, separate treatment as two events is justified: if for the first one $\delta B_\parallel/\delta B_\perp = 0.2 \div 0.3$, the second one is, as already observed by Tsurutani et al. (2002), an incompressible wave with $\delta B_\parallel/\delta B_\perp \propto 0.1$ and $\vartheta_{Bk} \approx 19°$, i.e. quasi-parallel in its propagation direction. The ratio of the intermediate to minimum eigenvalues of the minimum variance analysis (MVA) of the event is $\lambda_2/\lambda_3 = 4.2$, while the respective quantities for the first of the events are $\vartheta_{Bk} \approx 34°$ and $\lambda_2/\lambda_3 = 3.5$.

The next feature in which these two, otherwise adjacent wave trains, differ substantially is the sense of rotation of their field vector in minimum variance coordinates. The ellipticity is positive for the first and negative for the second event, i.e. the phase slip occurring at 08:19:45 is also accompanied by a change in the sense of rotation of the field vector. The ellipticity properties of the two events are illustrated in the two hodograms in Fig. 2a. The hodogram on the left-hand side belongs to the first of the events, while the right-hand side one represents the second wave sequence. The peak-to-peak amplitudes of the waves amount to only $\approx$0.15 nT and $\approx$0.30 nT, respectively, which means that with only about 1–2 percent modulation of the background field the disturbances of the medium have a strictly linear character. It is obvious from the temporal representation in Fig. 2a that both events have practically identical wave frequencies and these are to a good approximation equal to half the local proton cyclotron frequency – a property which we are going to have a closer look at when we come to the interpretation of the waves.

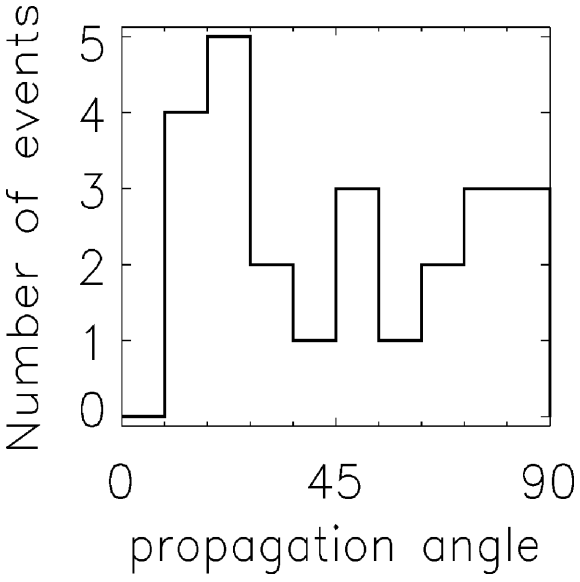

Fig. 3. Distribution of the propagation direction of the waves (minimum variance direction) with respect to the background magnetic field.

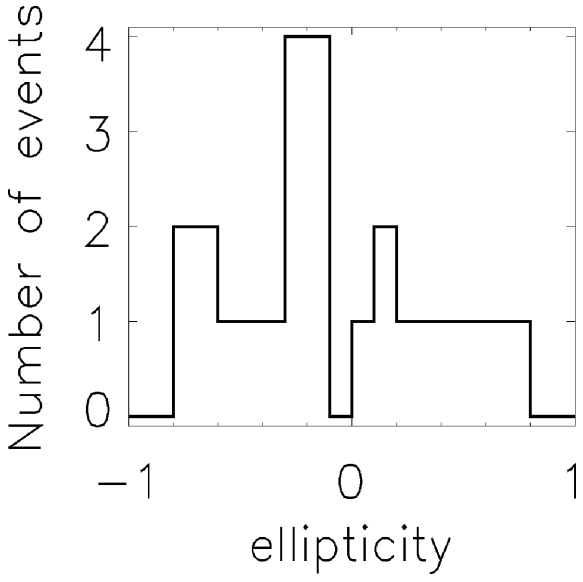

Fig. 4. Ellipticity distribution: the ratio of the eigenvalues λ_2/λ_1 in the plane perpendicular to minimum variance is taken as a measure of the ellipticity of the waves; positive/negative values are assigned to right-hand/left-hand rotating magnetic field vector projection in the plane defined above with the angle between the minimum variance direction and the average magnetic field confined to the 0°–90° range.

The next example, Fig. 2b, is a specimen of a short wave sequence observed in the time 09:52:07–09:52:33 UT. This event, similar to the first one in Fig. 2a, is right-hand polarised and has a clear pattern of a transverse wave propagating at some 30° off the main field, with a frequency that is at half the rotation rate of the protons in the background magnetic field. Different from the almost uninterrupted succession of wave events observed in the time around 08:19 UT (Fig. 2a) for an interval which lasts about 5–6 min, here the wave event is a lonely interruption in the otherwise unstructured wave activity of this period.

The waves in the following two examples no longer obey our selection criterion, which demands that λ_2/λ_3 be larger than 3. We need them, however, to obtain a closed picture of the observations.

In Fig. 2c the wave sequence between 10:03:15 and 10:03:35 UT is presented – an example of a wave with a substantial compressional component. A value of $\lambda_2/\lambda_3 = 1.5$ makes the MVA not very persuasive. This is why the hodogram in the MVA representation is not a very good indicator for the real wave properties. We should look rather at the time series representation in GSM reference system from which one can readily see that the x-component carries practically the whole of the background field, and the longitudinal and transverse wave components have comparable peak-to-peak amplitudes of about 0.15 nT. The compressional component mounted on the background magnetic field has a frequency of 0.14 Hz, while the cyclotron frequency of the protons locally amounts to 0.18 Hz. The question is, however, whether the proximity of the two numbers is not misleading: the wave observed here could be the result of the spacecraft crossing a region with a mirror mode structure, which could produce the observed signature of compressional wave mode in the longitudinal magnetic field fluctuations (cf. Tsurutani et al., 1984). Obeying our criteria, this type of wave (longitudinal) is not included in the statistics, and we do not discuss further this kind of mode.

The last of the examples, Fig. 2d, (10:10:37–10:11:07 UT) is shown in order to emphasise that wave sequences, which at a first glance have a good chance of fulfilling the criteria of the analysis, do not really contribute to the wave statistics that we are going to discuss in the next step. The reason, as with the wave in Fig. 2c (the compressional case), lies in the low value of the λ_2/λ_3 parameter, which is here ≈ 2.

3.2 Wave statistics

The results of the statistical treatment are summed up in Figs. 3–6. We have investigated the waves for the behaviour of their most important parameters and for the correlations of the latter. As already explained, we study only those events for which the quality criterion of the MVA, the ratio of the intermediate to the minimum eigenvalues λ_2/λ_3, is larger than 3. In such a way, we exclude a priori the waves with clearly longitudinal structure, since the latter correspond as a rule to $\lambda_2/\lambda_3 \leq 3$. This means that the results below characterise only the subset of the quasi-transverse waves.

As obvious from Fig. 3, modes running quasi-parallel to the background magnetic field B_0 are in balance with modes quasi-perpendicular in their propagation direction. In all instances where the term "propagation angle" appears, the angles between 90° and 180° have been folded onto the interval 90–0°, keeping in mind that the minimum variance

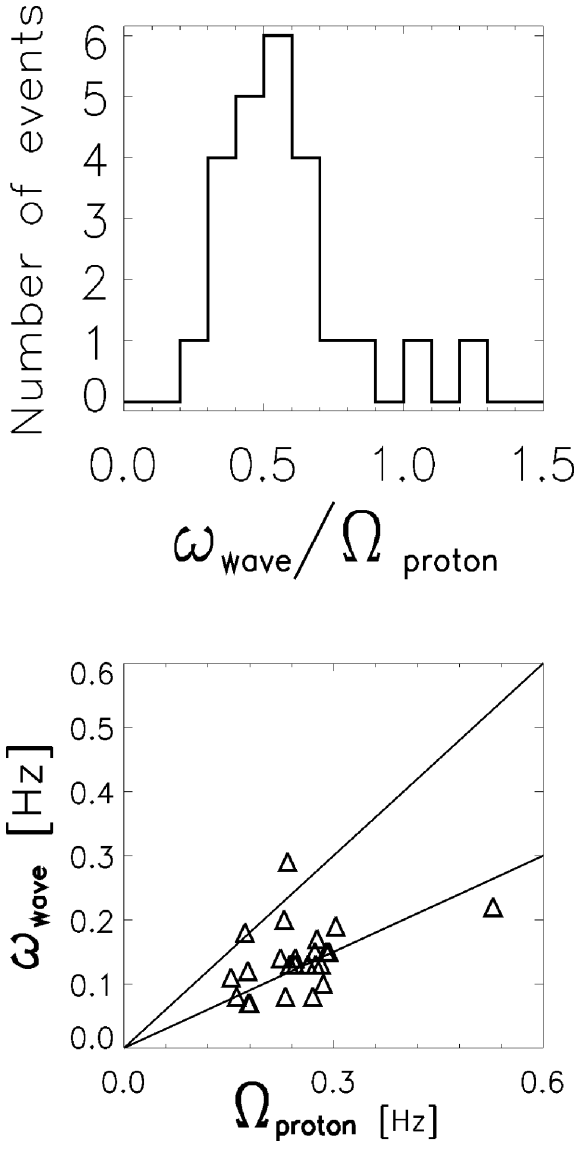

Fig. 5. (a) Histogram and **(b)** scatter plot of the distribution of the wave frequency normalised to the local proton cyclotron frequency. See details in the text.

method comes short of determining the absolute direction of propagation (single spacecraft measurement limitation). The empty 0–9° bin could be due to two reasons. One is a simple binning effect coming from the too narrow interval chosen (too low statistics). The absence of observations there could be, however, an indication that we are observing mainly waves that do not belong to the guided mode dispersion surfaces, but rather belong to the non-guided ones, the latter having no pronounced increment maximum at parallel propagation, cf. Denton et al. (1996).

The polarisation properties are summarised in the histogram in Fig. 4. Waves of negative ellipticity (values near to -1), i.e. left-hand polarised, are almost balanced by right-hand rotating modes (values around $+1$). Waves of linear ($|\lambda_2/\lambda_1| < 0.3$) rather than circular (values of $|\lambda_2/\lambda_1| > 0.6$) polarisation dominate. We are going to see in the discussion that the dominance of linear polarisation is a feature which is not so easy to reconcile with theory.

The frequency distribution of the waves is illustrated in Fig. 5, where a maximum at about half the local proton cyclotron frequency can be identified. The frequencies given here are in the s/c reference system. The relevance of these data for understanding the real plasma properties is discussed in the next subsection.

We examine next the correlation between the major wave parameters. The dependence of the propagation angle on the quality criterion of the MVA, λ_2/λ_3 is illustrated in Fig. 6a. It can be readily seen that for values larger than 7–8, the wave vectors become highly parallel to the background field $\boldsymbol{B_0}$. For $\lambda_2/\lambda_3 \leq 5$ the propagation direction becomes uniformly distributed over the whole interval of angles between 0° and 90°, which is partially also due to the fact that the smaller the quality parameter, the lower the accuracy of determining the minimum variance direction. No clear correlation can be found between the propagation angle of the waves and their ellipticity and frequency distributions (Figs. 6b and c). The different propagation directions seem to be evenly represented with respect to these two properties. In Fig. 6d, the correlation of the frequency to the ellipticity is plotted and again no clear trend is visible.

In Fig. 7, the evolution with time of three of the wave parameters is presented. In the first plot, the propagation direction derived from minimum variance analysis exhibits no clear pattern, in order to be able to distinguish between influences of different plasma environments. On the surface, a tendency of a transition from quasi-perpendicular to quasi-parallel propagation with time is observable. The spread in the data does not allow, however, for this trend to be quantified.

With the normalised wave frequency, as one should have expected, nothing spectacular happens with time because of the narrow distribution around $\Omega_p/2$. The time signature of the ellipticity in the lowermost panel of Fig. 7 is most irregular compared with the former two characteristics, and this makes it less suitable for drawing physically meaningful conclusions.

3.3 Uncertainties in wave properties, due to the lack of plasma measurements

Without having the plasma convection speeds, as in our case, the wave modes cannot be uniquely identified. We have no other choice but to prove indirectly whether this deficiency could be a source of grave errors. That this does not introduce substantial distortions in the frequency analysis is best seen from the character of the distribution curve (Fig. 5), which is centred on a narrow frequency band around $\Omega_p/2$, of only 0.2 half-width. If we remember now that the events included in the statistics originate from a magnetotail interval spanning about 30 R_E, which by no means can offer a uniform background of convection velocities, it becomes clear that the observed peak would not have been possible if the scat-

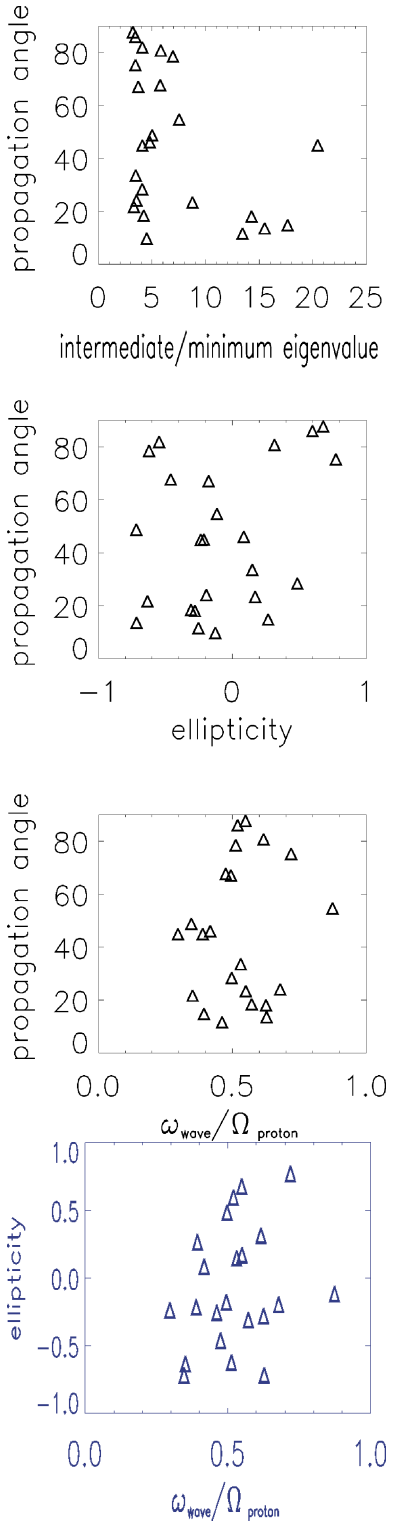

Fig. 6. Results from minimum variance analysis: propagation angle vs. **(a)** λ_2/λ_3, intermediate to minimum eigenvalue ratio as criterion for the quality of the MVA, only $\lambda_2/\lambda_3 > 3.0$ events are accounted for; **(b)** ellipticity and **(c)** wave frequency; **(d)** wave frequency vs. ellipticity.

tering in frequency through Doppler shifts would have been of substantial importance. In other words, accounting for the Doppler shift formula, one can make the indirect conclusion that during the observation period the prevailing magnetotail conditions did not support large plasma convection velocities, i.e. $V_{\rm conv}/V_A \leq 0.1-0.2$. Thus, the whole of our further discussion is based on the premise that the plasma convection speeds are not essential; hence, the observed frequencies do not substantially deviate from those in the reference system of the plasma medium. In the following, one should be aware of the uncertainty of the interpretation, which stems from the described limitations and which are further clarified in the discussion.

4 Wave properties – discussion

We address now the question about the origin of the waves. It is well known that the ion cyclotron frequency interval is the host of waves on the Alfvén and magnetosonic branches. In particular, the vicinity of the ion cyclotron resonance is of special importance in media characterised by anisotropic ion temperatures. In this range ion cyclotron waves are favoured, with their excitation mechanisms being intimately linked to the existence of ion beams and non-equilibrium ion velocity distributions (Gomberoff and Neira, 1983).

Comparison of the dispersion relation of plausible plasma configurations with the results of the data analysis is one of the possible ways to solve the problem. Our observations, carried out in the magnetotail as far out as 60 R_E, concentrate on low frequency wave burst activity of a type which has been discussed in depth by many authors. A variety of modes is possible, in principle. One of the main lines of distinction is whether the waves are dominated by a single ion species (Brinca et al., 1990; Chaston et al., 1994, 1999) or interplay of multiple ion components should be invoked (Smith and Brice, 1964; Young et al., 1981; Gomberoff and Neira, 1983; Kozyra et al., 1984; Brinca et al., 1989). Based on wave data only, we shall have to question both hypotheses.

Tsurutani et al. (2002) and Southwood et al. (2001) have already pointed out, without going into further detail, the specific property of the wave frequency distributions to peak around half the gyrofrequency of the protons. From our statistical analysis, cf. Fig. 5, this feature is more than obvious. Also accounting for the polarisation properties – the peak in the ellipticity distribution, Fig. 4, we discuss first the possibility of a multi-ion medium as the source of the waves.

4.1 Plausible plasma configurations

In a plasma with protons as the majority species and an observable presence of a heavy ion component, the dispersion properties are substantially modified in comparison to those in the case of a single ion species plasma. New modes come into play, producing a more or less complex picture of the wave dispersion, depending upon the thermal properties of the constituent ion species. The general dispersion behaviour

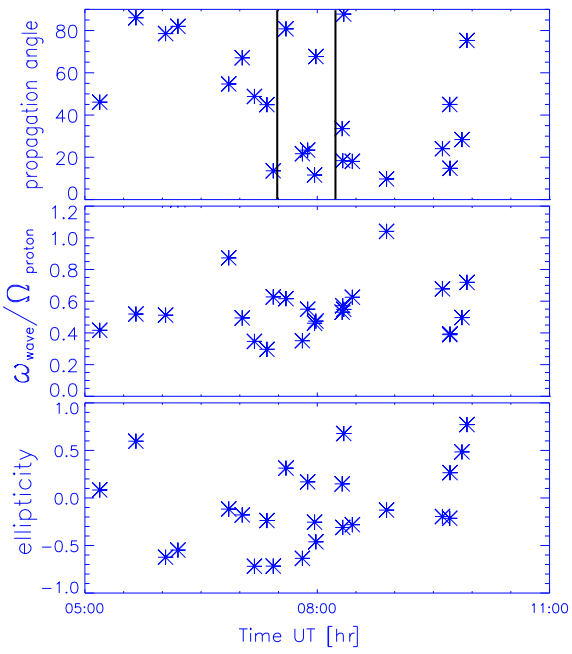

Fig. 7. The distribution in time (or along the trajectory) of parameters of the events including the propagation angle, normalised wave frequency, and ellipticity. The two vertical lines represent the approximate transition times between periods of possibly different propagation direction patterns, as explained in the text.

of such plasmas has been studied extensively, for example, by Andre (1985). For our purposes we have to be more specific, however, and shall keep close to studies concerning plasmas relevant for the Earth's magnetotail.

One option has been exhaustively investigated in works of Gomberoff and Neira (1983) and Kozyra et al. (1984) on the instability properties of plasmas with one or more warm anisotropic ion components and at least one cold ion species for the case of parallel propagation. There, the existence of narrow instability bands just below the heavy ion cyclotron frequency and possibly stop bands on its other side has been demonstrated, and the convective growth rates for the most unstable modes have been calculated. Whether the waves in the immediate vicinity of the heavy ion gyrofrequency are convectively enhanced and how large their growth rates are, depends in a complicated way on the anisotropy ratio $T_\perp/T_\parallel$ of the warm proton component (single warm ion species) and the abundance ratio of the cold heavy ions (Kozyra et al., 1984).

An idea about the properties of such systems is given by the relatively clear picture in the limit of a bi-ion plasma of warm anisotropic protons and cold minority species of He^{++} ions, Fig. 8. A new resonance, additional to the proton one, appears at the heavy ion cyclotron frequency Ω_h and a temperature independent cutoff emerges at $\omega_{co} = \Omega_h(1 + M_h N_h)/(1 + N_h)$, where M_h, N_h are the heavy ion mass and density in units of the dominant species of bi-Maxwellian distributed light ions (e.g. protons). The new intermediate left-hand polarised branch, starting at ω_{co}, reaches a resonance at Ω_p, the proton gyrofrequency, and crosses, at strictly parallel propagation (not shown here), the right-hand polarised branch at the crossover frequency $\omega_{cr} = \Omega_h[(1+N_h M_h^2)/(1+N_h)]^{1/2}$. At non-parallel propagation, the latter marks the point where the oppositely polarized branches merge and the polarisation goes through linear over a narrow k-interval. An illustration is given in Fig. 8 for the case of propagation 10° off the ambient magnetic field. The plots on the left-hand side depict the dependence of the normalized frequency and growth rate (curves denoted with γ) on the magnitude of the wave vector $\boldsymbol{k}$, normalized by the proton gyroradius. The right-hand side plots show the polarisation of the magnetic fluctuations δB_x, δB_y (e.g. Gary and Cairns, 1999), defined by the real part of $P(k) = i\delta B_x/\delta B_y \,\mathrm{sign}(\omega_r)$, with the wave vector $\boldsymbol{k} = \hat{y}k_y + \hat{z}k_z$ and $\boldsymbol{B_o} = \hat{z}B_o$; values of $+1/-1$ mean right-hand/left-hand polarised waves, respectively, while absolute values $\gg 1$ and around zero indicate linear polarisation. The He^{++} abundance is assumed to be 5% of the proton number density. This is a good approximation of the usual ratio in the solar wind, Hundhausen (1995), and in the magnetotail, Seki et al. (1999). The proton and electron parameters, given in the figure caption, represent a simplified model for magnetotail conditions. Three solutions are possible under these conditions. The uppermost plots present the left-hand polarised wave emerging from the cutoff frequency and merged in the crossover point ($k R_{\mathrm{protons}} \sim 0.11$), with the high frequency portion of the right-hand polarised branch. The middle row shows the complementary pair of modes which come together in the crossover point as a result of the non-parallel propagation: the low frequency part of the right-hand polarised branch, merging with the left-hand polarised branch, which tends to the proton cyclotron resonance in the short-wave limit. The lowermost plots reflect the behaviour of the purely left-hand polarised mode, which asymptotically approaches the gyrofrequency of the heavy ion component. Under these conditions, on both sides of the heavy ion (He^{++}) resonance frequency, wave generation is possible. The growth rates on the purely left-hand polarised branch (lowermost row) are noticeably lower than those on the branch limited by the proton resonance frequency (middle row). The unstable regions are on both sides and in a narrow interval around the He^{++} resonance frequency. It is obvious that plasma configuration of this type can produce a signature in the wave spectrum as observed by CASSINI (Fig. 5). It exhibits linear polarisation, however, only in regions of the dispersion curves of negligible or no growth rate at all. We shall see later what implications this could have.

In the attempt to interpret our observations, the key question is how complex are the assumed multi-ion plasmas. There is experimental evidence that the He^{++} ions found in the magnetotail have thermal velocities on the order of those of the protons, Lennartsson (2001). Therefore, in a realistic approach one should assume that all ion components are hot and solve the full kinetic dispersion equation for anisotropic plasmas. Using the WHAMP-Code, Rönmark (1982), we

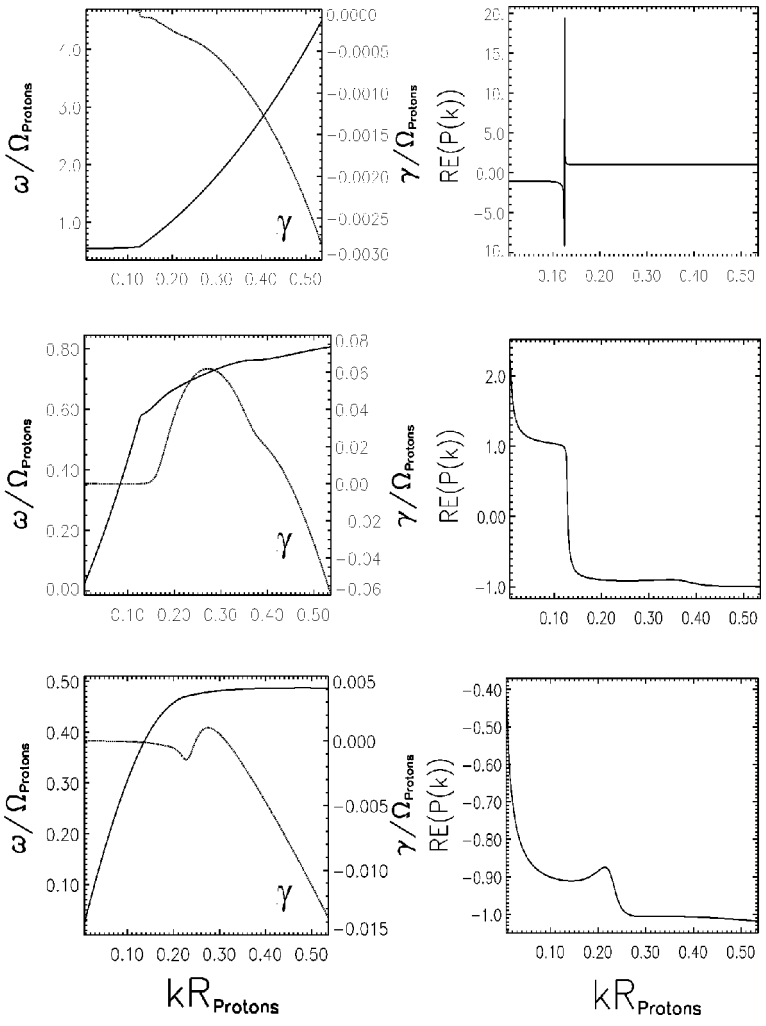

Fig. 8. Bi-ion cyclotron waves propagating 10° off the ambient magnetic field: dispersion in the presence of 5% of cold He^{++} on a background of hot anisotropic protons of $T_{p\perp}/T_{p\|} = 5$, $T_{e\perp}/T_{e\|} = 1$ and $T_{p\|} = 1.0\,10^6$ K, $T_{e\|} = 5.0\,10^6$ K, $N_p = 0.20\,\mathrm{cm}^{-3}$, $B_o = 10$ nT. The dispersion curves, $Re(\omega)$, and growth rate curves, $Im(\omega) \equiv \tilde{a}$, as a function of the wave number (module of the wave vector) normalized by the proton gyroradius, R_{protons}, are given on the left-hand side plots. The plots on the right-hand side represent the polarisation of the waves as defined in the text. The meaning of the different branches is discussed in the text.

Table 1. Normalised moment parameters for the ion and electron distributions used to calculate the dispersion relations in Fig. 9 and 10. (from Table 5 in Chaston et al., 1999)

Parameter	Protons	Electrons
n_j/n_t	1	1
$T_{\perp j}/T_{\| j}$	2.12	1.32
$T_{\perp j}/T_{\perp c}$	1	0.272
V_{oj}/V_A	−0.095	0.013

Here $n_t = 0.197\,\mathrm{cm}^{-3}$
$T_{\perp c} = 2749.1$ eV; $B_o = 10$ nT;

have studied the behaviour of such a plasma. We devise a realistic parameter set by taking a parameter combination as used in a study by Chaston et al. (1999), Table 1. We extend this set, however, by adding a warm isotropic He^{++} population, specified in the caption of Fig. 9. Zero drifts for all the particle species involved are assumed. After Lennartsson, (2001), for He^{++} ions of solar wind origin one has to assume parallel temperature approximately 4 times the temperature of the protons, $T_{\mathrm{He}^{++}\|}/T_{\mathrm{H}^{+}\|} \approx 4$. Then, for quasi-parallel propagation, $\theta_{Bk} = 10°$, only the branch below the heavy ion resonance frequency possesses a positive growth rate with a maximum at $\omega/\Omega_p \approx 0.45$, the lowest row of plots in Fig 9. The other two branches do not exhibit positive growth rates at all. One of them, shown in the middle row, starts at the cutoff frequency and has a hybrid polarization behaviour, determined by its passing over the cross-over point. There, it also crosses the third branch, plotted in the first row of Fig. 9. This one has right-hand polarization and exhibits no resonance at low wavelengths (large k-values), while the unstable branch is left-hand polarised in the interval of positive growth rates ($kR_{\mathrm{protons}} \approx 0.35 \div 0.65$), with polarisation values $Re(P(k)) \approx -0.70 \div -0.90$, i.e. quasi-circular polarisation. This behaviour is different from the case of plasma with a cold He^{++} component. There, the branch between the He^{++} and H^{+} cyclotron resonance frequencies contains a further interval of positive growth rates of values which make it dominant in the dispersion, and is separated from the lower frequency branch by a more or less narrow stop band, cf. Fig. 8. We see that replacing the cold

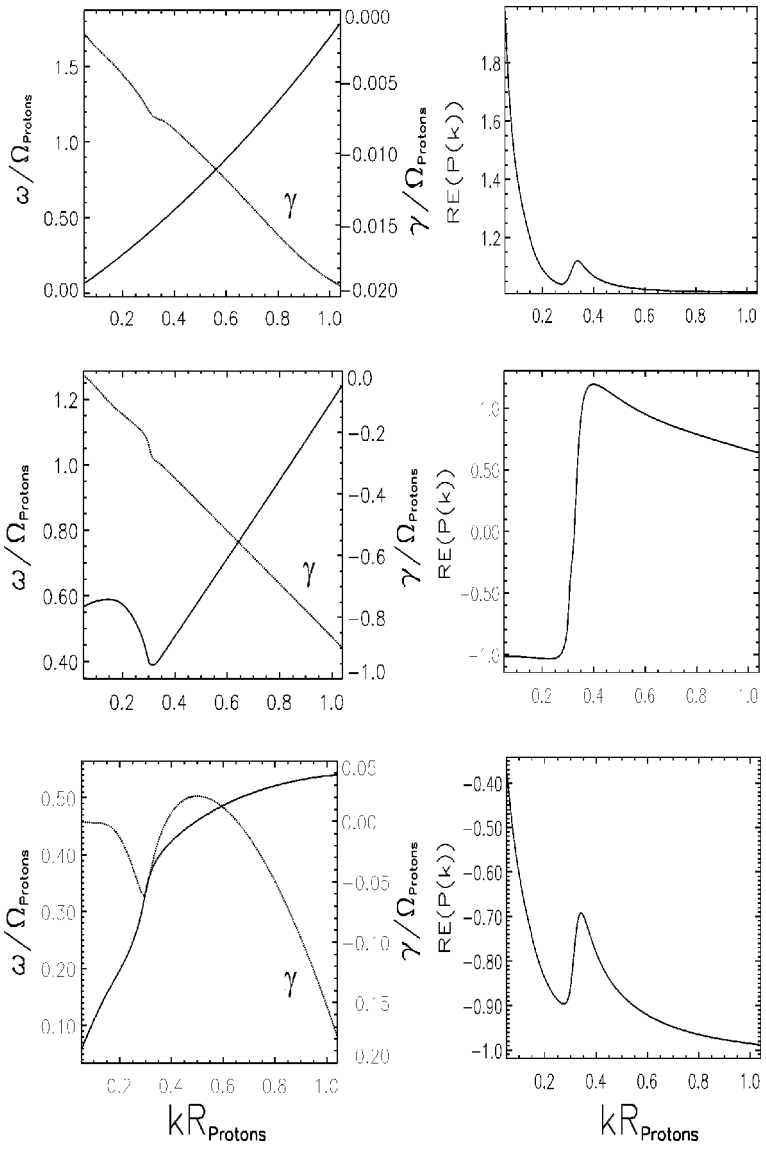

Fig. 9. Bi-ion cyclotron waves at quasi-parallel propagation ($\theta_{BK} = 10°$): dispersion in the presence of 5% of hot He^{++} on a background of hot anisotropic protons and electrons as in Table 1 (from Chaston et al., 1999); $T_{He^{++}\parallel}/T_{H^+\parallel} = 4$ and $T_{He^{++}\parallel} = T_{He^{++}\perp}$ (Maxwellian distribution of the He^{++} ions). For details, see the text. The notations are explained in Fig. 8.

He^{++} ions with a hot population radically reduces their influence on the dispersion of the plasma, with the protons becoming dominant. This will be obvious, when we come to the last example of plasma with a single ion species. If we compare these properties with those of the observed waves, Fig. 4, it becomes obvious that the agreement between theory and experiment for the polarisation parameter is on a much lower level than in the case of the frequency distribution of the waves. This could be understood in the light of results by Denton et al. (1996). They have shown that under similar conditions, the superposition of two pure wave states of similar polarisation characteristics tends to produce an observable polarisation, which is closer to linear than the polarisations of the constituent waves. The implication is that the single wave model, which we are using, is far from being perfect. With the data volume at hand, however, we do not have a better alternative.

A further bi-ion plasma possibility would be the presence of He^+ ions (with mass per charge ratio of $M_h/Q_h = 4$) in abundance, which is enough to produce a cross-over frequency $\omega_{cr} = \omega_{He^+}(1 + 15N_{He^+}/N_{total})^{1/2}$ on the order of half the proton cyclotron frequency. This option cannot be excluded a priori because of the well-known enrichment of the plasma sheet in He^+ ions of ionospheric origin during substorm activity. With He^+ abundances on the order of 10%, as observed in the magnetotail (Young et al., 1981; Seki et al., 1999), we have $\omega_{cr} \approx 1.6\Omega_{He^+} \approx 0.40\Omega_{H^+}$. This means that if a bi-ion spectrum with cold He^+ is at work, two options are possible. Either a spectral peak around this value should be expected, accompanied by a relatively well pronounced gap between 0.25 Ω_{H^+} and 0.33 Ω_{H^+} (the value of ω_{co} for this case), or if the He^+ concentrations are lower, the gap will be closed but the spectral peak will slide towards even lower frequencies close to the ω_{He^+} resonance. A problem with this interpretation is that the relatively sharp peak observed around the value of $0.5\Omega_{H^+}$ cannot be convincingly

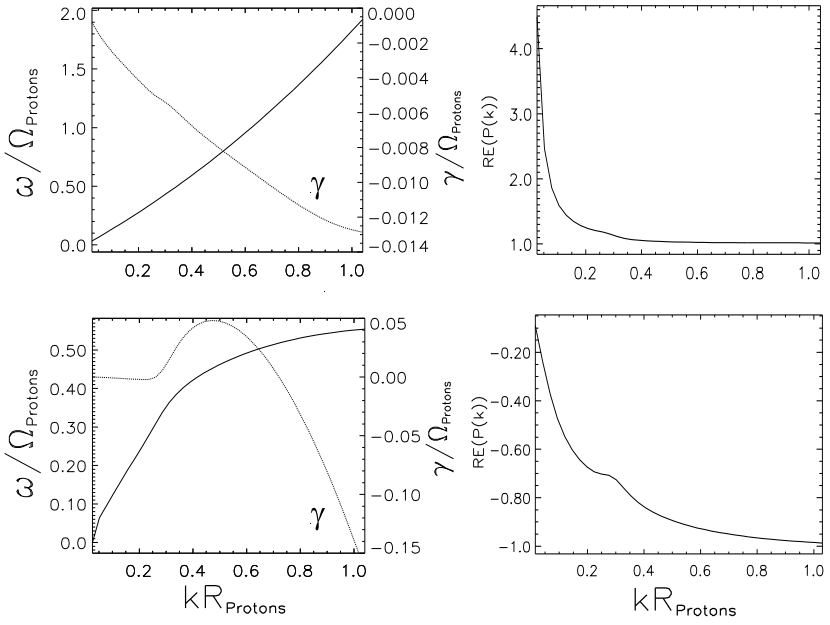

Fig. 10. Dispersion curves for a bi-Maxwellian plasma distribution function with parameters as those used for Fig. 13 from Chaston et al. (1999), our Table 1; different is only the propagation direction 10° off the background magnetic field. The growth rate on the Alfvén branch reaches a maximum for values of the wave frequency in the narrow interval around $\Omega_p/2$. The curves with the right-hand polarisation describe the magnetosonic branch, which is not enhanced under these conditions. The notations are explained in Fig. 8.

explained.

We turn now to an alternative interpretation: waves excited in plasma with only one ion species (protons) as, for example, in works by Brinca et al. (1990) on proton induced waves downstream of the bowshock, or by Chaston et al. (1999) dealing with the dispersion properties of electromagnetic ion cyclotron (EMIC) waves in the near-Earth magnetotail. In the latter, the authors have demonstrated, under the restriction $\boldsymbol{k} \times \boldsymbol{B_0} = 0$, that in the magnetotail plasma sheet, conditions exist which are favourable for the excitation of EMIC waves. In particular, the Alfvén branch can be excited and the growth rates of the waves reach a maximum in the frequency band around half the proton cyclotron frequency. In Fig. 10 the dispersion properties of plasma with parameters similar to those used by Chaston et al. (1999) for his example of plasma sheet waves are plotted with the modification of $\theta_{Bk} = 10°$, instead of strictly parallel propagation. A glance at the dispersion curves shows that a bi-Maxwellian distribution of the proton velocities ensures positive growth rates on the Alfvén branch in the frequency range just below the $\omega/\Omega_p = 1/2$. The proton and electron distribution parameters used to derive the dispersion curves in Fig. 10 and characteristic for the magnetotail plasma sheet are given in Table 1. (cf. Table 5 in Chaston et al., 1999). As explained in this work, essential for the energy release in the form of Alfvén waves, for the form of the instabilities and of the dispersion curves is the anisotropy, even in its very weak form assumed here (Table 1), and not the relatively weak drifts of the proton and electron populations observed in the plasma sheet of the magnetotail. Here, again, while the theoretical and experimental frequency distributions agree relatively well, the left-hand circular polarisation prescribed by theory (see the lower right-hand polarisation diagram in Fig. 10) for the growing waves is not followed by the observation. We can now compare the features of the unstable modes, lowermost plots in Figs. 9 and 10. It is easy to see that, as already hinted to, there are only minor differences, i.e. the presence of a minor component of hot, heavy ions does not substantially disturb the form of the curves of the modes which are most probable to be observed in experiments.

Obviously neither of the two hypotheses (single- or multi-ion plasmas) provides a satisfactory explanation for the peak at linear polarisation. A possible reason for the discrepancy could lie in the fact that we observe the waves after they have propagated away from their source region and have undergone a polarisation evolution from circular to linear, as discussed in the work by Rauch and Roux (1982). They have shown that in the case of a cold, heavy ion component (He^+) and anisotropic protons the originally circularly polarized bi-ion cyclotron waves could acquire linear polarisation when moving into plasma, for which their normalized frequency approaches the local cross-over frequency. Their study envisages a case of guided wave propagation in the equatorial magnetosphere at $L \approx 7$, while we have magnetotail conditions with a heavy ion component, which, as already mentioned, cannot be treated as cold. Whether this mechanism is effective under such conditions is under investigation and is beyond the scope of this paper.

Keeping in mind that heavy ion populations in the Earth's magnetotail exist mainly in the form of beams, it is legitimate to ask whether beam type instabilities could be the source of the observed waves. A potential candidate could be the ion-ion resonant right-hand instability, which can produce waves in the same frequency range (Gary et al., 1984, 1985, 1987; Tsurutani et al., 1985; Kawano et al., 1994). They would have, however, a polarisation, which is quite different from what we see in the experiment. There is a further obstacle to this explanation: the threshold velocity of the

beam for the instability to develop is $V_{\rm beam} \geq V_A$, which is rather not the case under magnetotail conditions (Seki et al., 1999; Lennartsson, 2001), especially for the CASSINI range of magnetotail observations with $X_{\rm GSM} = -20 \div -60\,R_E$, where beam velocities of about 50–100 km/s were measured, and where Alfvén velocities of at least several hundred km/s are the rule. Also to note, is that for the ion-ion resonant right-hand instability, the beam velocity threshold condition does not change substantially with growing beam temperature anisotropy. On the contrary, the behaviour of the ion cyclotron beam anisotropy instability is quite different. While isotropic beams are stable, non-zero anisotropy of the beam temperature produces positive growth rates, beginning already with zero drift velocities, Gary and Schriver, (1987). If we account for the left-handedness of the polarisation of this instability, however, we still have the problem with explaining the ellipticity properties of our data.

A similar check with the low frequency kink-like instability, which was studied for the plasma sheet boundary layer by Angelopoulos et al. (1989), shows that for typical PSBL conditions this instability has positive growth rates for frequencies $\omega \ll \Omega_p$, which lie well below our range of $\omega/\Omega_p \approx 0.5$. For this reason it is irrelevant for our investigation.

5 Conclusion

In summary, the frequency histogram, Fig. 5, with the peak of the distribution lying just above the He^{++} gyrofrequency, would agree with both plasma of anisotropic bi-Maxwellian protons, with a warm minority He^{++}-species (Fig. 9), or with plasma composed exclusively of protons with appropriate anisotropy values, as in Fig. 10. We need further criteria to discern between these two possibilities. The observed polarisation behaviour of the waves, with the maximum of the ellipticity distribution in the interval of small negative values (linearly polarised waves, Fig. 4), is in contrast with the theoretical polarisation for any of the conceivable plasma configurations, if we really observe the waves at their generation site, i.e. without any further modifications. If, on the contrary, we assume that they have undergone some propagation, this discrepancy becomes an implicit argument for the He^{++} case, because only in the presence of a heavy ion component does linear polarisation emerge and this type of transition becomes principally possible. One more reason for favouring the bi-ion He^{++} hypothesis is that any other type of mechanism would, with the substantial scatter of plasma parameter values, which we have between 20 and 60 R_E, produce no distinguishable peak in the frequency distribution of the waves.

Again, however, we should not forget the alternative explanation discussed in the section on plausible plasma configurations, that wave superposition, also in the case of single ion plasma, could result in observed polarisations much more linear than one would expect, judging only on this parameter of the individual modes.

The idea of a bi-ion plasma excitation mechanism is also supported by existing magnetotail plasma observations, since ISEE – I times He^{++} ions have been known to be a constituent of the magnetotail plasma at least up to distances of 23 R_E, Lennartsson and Shelley (1986). It has not been very long now, however, that data are available indicating the presence of low concentrations of solar wind He^{++} ions in the deep magnetotail, as far away as 200 R_E, (Seki et al., 1996; Lennartsson, 2001). These are a permanent constituent of the solar wind and can penetrate the magnetotail, together with the main component – the H^+ ions. According to the formula for the cutoff frequency, precisely the case of vanishing abundance of the heavy ion species (about 5% in number density, on the average) produces a cutoff at practically the cyclotron frequency of the latter: $\omega_{co} \cong \omega_{\rm reson} = 0.5\Omega_{\rm H^+}$. Thus, the forbidden band for the left-hand polarised waves between the heavy ion gyrofrequency and the cutoff frequency practically vanishes (Fig. 8). Waves of both polarisations then become possible over the whole frequency range on both sides of $\Omega_{\rm He^{++}}$. The problem with this is again, that with realistic He^{++} temperatures only the lowest frequency branch is unstable, Fig. 9, and the difference between waves in single-ion and multi-ion plasma becomes smeared (compare Fig. 9 and Fig. 10).

We already know, cf. Sect. 2, and Khan et al. (2001), the periods within which CASSINI was in the plasma sheet and in the northern magnetotail lobe, respectively. The encounter with ion cyclotron waves of the type discussed here along almost all of CASSINI's magnetotail passage (Figs. 1 and 7) makes it, however, impossible to use them as an unambiguous criterion for the type of plasma environment within which the waves were observed. Why they should persist in both the plasma sheet and in the lobes, two plasma media that have substantially different characteristics, can be answered only in a further work correlating the magnetic field data with the plasma measurements.

The time dependence of the propagation angle could also give us a clue to the site of origin of the waves. In Fig. 7a the transition from quasi-perpendicular to quasi-parallel propagation at about 08:00 UT can be traced, although the statistics is not enough to clearly substantiate this difference of behaviour between the first and second half of the magnetotail period. This change in the wave characteristics coincides with the time when the s/c enters the magnetotail lobe, a plasma medium of very low density, compared with the plasma sheet and the PS boundary layer. A possible explanation of the change in the propagation mode could be the assumption that the prevailing conditions in one of these plasma media do not promote the local excitation of the observed waves and their appearance in this region is due to their transport hitherto via wave-guiding phenomena. Such interpretation, where we assume that the waves are partially observed not at the site of their generation, but after they have travelled over some propagation distance, as is usual in ray-tracing problems, requires the fulfilment of certain conditions. As shown in Rauch and Roux (1982), the presence of minor ion components, in our case this is He^{++}, can sub-

stantially change (enhance) the wave-guiding properties of the plasma medium. Abstaining from analysis of the particle data, as is the case here, it would be highly speculative, however, to follow further this line of reckoning.

6 Summary

Analysing the low frequency magnetic field fluctuations observed by CASSINI in the magnetotail, we have found that they can be identified as waves of the ion cyclotron type, characterized by the following two qualities: a relatively narrow distribution of their frequency around the value of $\omega/\Omega_p = 0.5$ and a peak in the domain of linearly polarized waves. We have no relevant plasma convection velocity and minor ion density data for the observation interval. To overcome this obstacle we have projected the two key features on the theoretical predictions for the most plausible magnetotail plasma configurations. As a result, we argue that the observed waves could be the product of the joint action of the primary component of the magnetotail plasma – weakly anisotropic energetic protons, influenced in their instability by the presence of a minor species, He^{++} ions of solar wind origin. According to well-established theoretical understanding, this bi-ion system can support waves near the He^{++} cyclotron resonance. The known property of the He^{++} ions to have parallel thermal velocities equal to those of the protons makes this influence, however, very subtle. Thus, based on a limited data set like ours, one cannot definitely give preference to the bi-ion mechanism over the single ion hypothesis, in which the waves are produced alone by the action of the protons, on the Alfvén branch of the anisotropic ion cyclotron instability.

The attempt to exclude one of the two options based on the fact of dominant linear polarisation is also inconclusive because the initially circularly polarized waves can become or appear as linearly polarized for two reasons. On the one hand, they can undergo a transformation from circular to linear during propagation in a bi-ion medium and thus acquire properties which are in reasonable agreement with our observations. On the other hand, there exists work showing that linear polarisation could be the artifact of superposition of circularly polarized modes. The lack of supporting plasma data does not allow us to claim that either one of the two explanations can be uniquely favoured.

The waves appear in irregular intervals during the whole magnetotail period. Only a relatively small part of this time, however, can be related to coherent wave sequences, which means that larger plasma regions with the necessary anisotropy/ion beam properties are rather the exception in the background of otherwise actively wave emitting magnetotail plasma. Possible extension of this work should take place to find out to what degree the available plasma observations could be used in support of either interpretation. A further question is whether these allow for a closer survey of the propagation conditions of the waves, so that the indications of change in the average propagation direction at the transition from the plasma sheet into the lobe can be physically substantiated or refuted.

Acknowledgements. The work by ATB, KHG and GM was financially supported by the German Ministerium für Wissenschaft und Bildung and the German Zentrum für Luft- und Raumfarhrt under DLR Contract 50 OH 9901. Portion of this work was done at the Jet Propulsion Laboratory, California Institute of Technology, under contract with NASA. The authors acknowledge also the work of all the CASSINI staff engaged in the data retrieval and processing. We thank also Dr. Gunnar Paesold for supplying us and helping with the implementation of the latest version of the WHAMP-Code.

Topical Editor T. Pulkkinen thanks H. Koskinen and another referee for their help in evaluating this paper.

References

Anderson, B. J., Denton, R. E., and Fuselier, S. F.: On determining polarization characteristics of ion cyclotron wave magnetic field fluctuations, J. Geophys. Res., 101, 13 193–13 213, 1996.

Andre, M.: Dispersion Surfaces, J. Plasma Physics, 33, 1–19, 1985.

Angelopoulos, V., Elphic, R. C., Gary, P., and Huang, C. Y.: Electromagnetic instabilities in the plasma sheet boundary layer, J. Geophys. Res., 94, 15 373–15 383, 1989.

Bauer, T. M., Baumjohann, W., Treumann, R. A., and Sckopke, N.: Low-frequency waves in the near-Earth plasma sheet, J. Geophys. Res., 100, 9605–9617, 1995.

Brinca, A. L. and Tsurutani, B. T.: Influence of Multiple Ion Species on Low-Frequency Electromagnetic Wave Instabilities, J. Geophys. Res., 94, 13 565–13 569, 1989.

Brinca, A. L., Sckopke, N., and Paschmann, G.: Wave Excitation Downstream of the Low-β, Quasi-Perpendicular Shock, J. Geophys. Res., 95, 6331–6335, 1990.

Cattell, C. A., Mozer, R. S., Anderson, R. R., Hones, Jr., E. W., and Sharp, R. D.: ISEE observations of the plasma sheet boundary, plasma sheet and neutral sheet, 2, Waves, J. Geophys. Res., 91, 5681, 1986.

Chaston, C. C., Hu, Y. D., Fraser, B. J., Elphic R. C., and Huang, C. Y.: Electromagnetic ion cyclotron waves observed in the near-Earth plasma sheet boundary layer, J. Geomagn. Geoelectr., 46, 987, 1994.

Chaston, C. C., Hu, Y. D., and Fraser, B. J.: Non-Maxwellian particle distributions and electromagnetic ion cyclotron instabilities in the near-Earth magnetotail, Geophys. Res. Lett., 24, 2913–2916, 1997.

Chaston, C. C., Hu, Y. D., and Fraser, B. J.: Electromagnetic ion cyclotron waves in the near-Earth magnetotail, J. Geophys. Res., 104, 6953–6971, 1999.

Chaston, C. C., Hu, Y. D., and Fraser, B. J.: Quasi-linear ion cyclotron heating in the near-Earth magnetotail, J. Geophys. Res., 105, 5507–5516, 2000.

Denton, R. E., Anderson, B. J., Ho, G., and Hamilton, D. C.: Effects of wave superposition on the polarization of electromagnetic ion cyclotron waves, J. Geophys. Res., 101, 24 869–24 885, 1996.

Elphic, R. C. and Gary, S. P.: ISEE observations of low frequency waves and ion distribution function evolution in the plasma sheet boundary layer, Geophys. Res. Lett., 17, 2023–2026, 1990.

Gary, S. P., Smith, C. W., Lee, M. A., Goldstein, M. L., and Fooslund, D. W.: Electromagnetic ion beam instabilities, Phys. Fluids, 27, 1852–1862, 1984.

Gary, S. P., Madland, C. D., and Tsurutani, B. T.: Electromagnetic ion beam instabilities: II, Phys. Fluids, 28, 3691–3695, 1985.

Gary, S. P. and Schriver, D.: The electromagnetic ion cyclotron beam anisotropy instability, Planet. Space Sci., 35, 51–59, 1987.

Gary, S. P. and Winske, D.: Computer Simulations of Electromagnetic Instabilities in the Plasma Sheet Boundary Layer, J. Geophys. Res., 95, 8085–8094, 1990.

Gary, S. P.: Electromagnetic ion-ion instabilities and their consequences in space plasmas: A review, Space Sci. Rev., 56, 373, 1991.

Gary, S. P., Anderson, B. J., Denton, R. E., Fuselier, S. A., McKean, M. E., and Winske, D.: Ion anisotropies in the magnetosheath, Geophys. Res. Lett., 17, 1767–1770, 1993.

Gary, S. P. and Lee, M. A.: The ion cyclotron anisotropy instability and the inverse correlation between proton anisotropy and proton beta, J. Geophys. Res., 99, 11 297–11 301, 1994.

Gary, S. P., Convery, P. D., Denton, R. E., Fuselier, S. A., and Anderson, B. J.: Proton and helium cycotron anisotropy instability thresholds in the magnetosheath, J. Geophys. Res., 99, 5915–5921, 1994.

Gary, S. P. and Cairns, I. H.: Electron temperature anisotropy instabilities: Whistler, electrostatic and z-mode, J. Geophys. Res., 104, 19 835–19 842, 1999.

Gomberoff, L. and Neira, R.: Convective Growth Rate of Ion Cyclotron Waves in a H^+-He^+ and H^+-He^+-O^+ Plasma, J. Geophys. Res., 88, 2170–2174, 1983.

Hundhausen, A. J.: The Solar Wind, in: Introduction to Space Physics, edited by Kivelson, M. G. and Russell, C. T., Cambridge, Univ. Press, 1995.

Kawano, H., Fujimoto, M., Mukai, T., Yamamoto, T., Terasawa, T., Saito, Y., Machida, S., Kokobun, S., and Nishida, A.: Right-handed ion/ion resonant insatbility in the plasma sheet boundary layer: GEOTAIL observation in the distant tail, Geophys. Res. Lett., 21, 2887–2890, 1994.

Kellock, S., Austin, P., Balogh, A., Gerlach, B., Marquedant, R., Musmann, G., Smith, E., Southwood D., and Szalai, S.: Cassini dual technique magnetometer instrument (MAG), Proc. SPIE, v. 2803, 141–152, Cassini/Huygens: A Mission to the Saturnian Systems, (Ed) L. Horn, 1996.

Khan, H., Cowley, S. W. H., Kolesnikova, E., Lester, M., Brittnacher, M. J., Hughes, T. H., Hughes, W. J., Kurth, W. S., McComas, D. J., Newitt, L., Owen, C. J., Reeves, G. D., Dinger, H. J., Smith, C. W., Southwood, D. J., and Watermann, J. F.: Observation of Two Complete Substorm Cycles During the Cassini Earth Swing-By: Cassini Magnetometer Data in a Global Context, J. Geophys. Res., 106, 30 141–30 176, 2001.

Kozyra, J. U., Cravens, T. E., Nagy, A. F., and Fontheim E. G.: Effects of Energetic Heavy Ions on Electromagnetic Ion Cyclotron Wave Generation in the Plasmapause Region, J. Geophys. Res., 89, 2217–2233, 1984.

Lennartsson, O. W. and Shelley, E. G.: Survey of 0.1- to 16-keV/e Plasma Sheet Ion Composition, J. Geophys. Res., 91, 3061–3074, 1986.

Lennartsson, O. W.: Ion Composition Aspects of Magnetotail Plasma Flows, J. Geophys. Res., 106, 15 621–15 634, 2001.

Neagu, E., Gary, S. P., Borovsky, J. E., Baumjohann, W., and Treumann, R. A.: Constraints on magnetic fluctuation energies in the plasma sheet, Geophys. Res. Lett., 28, 919–922, 2001.

Rauch, J. L. and Roux, A.: Ray Tracing of ULF Waves in a Multicomponent Magnetospheric Plasma: Consequences for the Generation Mechanism of Ion Cyclotron Waves, J. Geophys. Res., 87, 8191–8198, 1982.

Rönmark, K.: WHAMP Waves in homogeneous, anisotropic, multicomponent plasmas, Rep. 179, Kiruna, Geophys. Inst., Kiruna, Sweden, 1982.

Seki, K., Hirahara, M., Terasawa, T., Shinohara, I., Mukai, T., Saito, Y., Machida, S., Yamamoto, T., and Kokubun, S.: Coexistence of Earth-origin O^+ and solar wind-origin H^+/He^{++} in the distant magnetotail, Geophys. Res. Lett., 23, 985–988, 1996.

Seki, K., Hirahara, M., Terasawa, T., Mukai, T., and Kokubun, S.: Properties of He^+ beams observed by Geotail in the lobe/mantle regions: Comparison with O^+ beams, J. Geophys. Res., 104, 6973–6985, 1999.

Smith, R. L. and Brice, N.: Propagation in Multicomponent Plasmas, J. Geophys. Res., 69, 5029–5040, 1964.

Sonnerup, B. U. O. and Scheible, M.: Minimum and Maximum Variance Analysis, in: Analysis Methods for Multi-Spacecraft Data, edited by Paschmann, G. and Daly, P. W., ISSI/ESA, 185–220, 1998.

Southwood, D. J., Dougherty, M. K., Balogh, A., Cowley, S. W. H., Smith, E. J., Tsurutani, B. T., Russell, C. T., Siscoe, G. L., Erdos, G., Glassmeier, K.-H., Gliem, F., and Neubauer, F. M.: Magnetometer Measurements from the Cassini Earth Swingby, J. Geophys. Res., 106, 30 109–30 128, 2001.

Tsurutani, B. T., Richardson, I. G., Lepping, R. P., Zwickl, R. D., Jones, D. E., Smith, E. J., and Bame, S. J.: Drift mirror mode waves in the distant ($X = 200\,R_E$) magnetosheath, Geophys. Res. Lett., 11, 1102–1105, 1984.

Tsurutani, B. T., Richardson, I. G., Thorne, R. M., Bugler, W., Smith, E. J., Cowley, S. W. H., Gary, S. P., Akasofu, S.-I., and Zwickl, R. D.: Observations of the right-hand resonant ion beam instability in the distant plasma sheet boundary layer, J. Geophys. Res., 90, 12 159–12 172, 1985.

Tsurutani, B. T., Arballo, J. K., Zhou, X.-Y., Galvan, C., and Chao, J. K.: Electromagnetic Electron and Proton Cyclotron Waves in Geospace: A Cassini Snapshot, in: Space Weather Study Using Multipoint Techniques, edited by Lyu, L.-H., Pergamon Press, 97–125, 2002.

Young, D. T., Perraut, S., Roux, A., de Villedary, C., Gendrin, R., Korth, A., Kremser, G., and Jones, D.: Wave-particle interactions near Ω_{He^+} observed on GEOS 1 and 2; 1. Propagation of ion cyclotron waves in He^+-rich plasma, J. Geophys. Res., 86, 6755–6772, 1981.